

On the Basins of Attraction of Parallel Connected Buck Switching Converters

Yuehui Huang and Chi K. Tse

Department of Electronic and Information Engineering, Hong Kong Polytechnic University, Hungghom, Hong Kong
<http://chaos.eie.polyu.edu.hk>

Abstract—This paper describes the coexisting attractors of parallel connected buck switching converters under a master-slave current sharing scheme. We present the basins of attraction of desired and undesired attractors, which provide design information on the conditions for hot-swap operations. The system employs a typical proportional-integral (PI) controller for regulation. It is shown that the system will converge to different attractors for different initial conditions with the same control parameters. Simulation results are given to illustrate the phenomenon. This study is relevant to practical design. Specifically we show that the stability regions obtained from linear methods (i.e., considering only local stability) can be over-optimistic as the global stability regions are found to be more restrictive in the parameter space.

I. INTRODUCTION

Power supplies based on paralleling switching converters offer a number of advantages over a single, high-power, centralized power supply. They enjoy low component stress, increased reliability, ease of maintenance and repair, improved thermal management, etc. [1], [2]. Since current sharing has to be maintained among the paralleled converters, some form of control has to be used to equalize the individual currents in the converters. One widely used method for balancing currents is the *master-slave current sharing* method [3], [4].

The system under study in this paper is a parallel connected system of two buck converters. Under the master-slave scheme, one of the converters is the master and the other is the slave. The master has a simple feedback loop, consisting of a typical proportional-integral (PI) control, to regulate the output voltage. The slave basically sets its current to equal that of the master via an active loop involving comparison of the currents of the two converters, as shown in Fig. 1. Previous studies of such systems have focused on pure proportional control [5], which is not normally used in practice. The use of PI control introduces a low-pass characteristic to the feedback loop, thereby suppressing high-frequency components in the feedback signal. The resulting bifurcation and stability behavior is therefore different. In this paper we will consider practical PI control in our simulation study.

Basically we find that for parallel connected converters, the desired operating orbit is not always reached from all initial conditions, even though the orbit has been found locally stable (e.g., from a linearized model). Depending on the initial state, the system may converge to a different attractor, which can be a limit cycle of a long period, quasi-periodic orbit or chaotic orbit. In this paper, we examine parallel connected buck

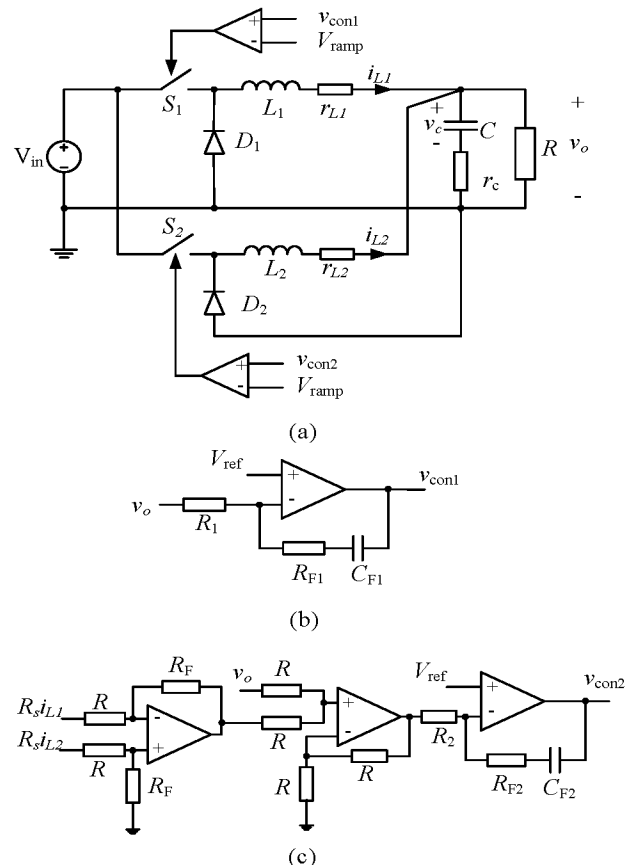


Fig. 1. Paralleled buck converters under master-slave control and PI control.

converters with PI control under master-slave current sharing. We show that different initial conditions may lead to different steady states. Thus, linear stability analysis methods, which basically evaluate the convergence of the system trajectory to the desired steady state starting from a nearby point, can be misleading. In this paper we report the phenomenon, present specific basins of attraction for the different attractors, and derive the critical values of control parameters for which the system loses stability of its expected operation. We generally observe that stability boundaries obtained from equivalent linear methods are over-optimistic, in that the system is actually more prone to instability. Thus, reliable stability information can only be obtained with the basin of attractions duly taken into consideration.

II. SYSTEM DESCRIPTION AND OPERATION

Figure 1 shows two buck converters connected in parallel [6]. In this circuit, S_1 and S_2 are switches, which are controlled by a standard pulse-width modulator which consists of a comparator comparing a control signal and a ramp signal. The ramp signal is given by

$$V_{\text{ramp}} = V_L + (V_U - V_L) \left(\frac{t}{T_s} \bmod 1 \right) \quad (1)$$

where V_L and V_U are the lower and upper thresholds of the ramp, respectively, and T_s is the switching period. Basically, switch S_i ($i = 1, 2$) is closed if $v_{\text{coni}} > V_{\text{ramp}}$ and is open otherwise.

The control signals v_{con1} and v_{con2} are derived from the feedback compensator, as shown in Figs. 1 (b) and (c). Here the compensator is a PI controller [7], e.g.,

$$\frac{V_{\text{con1}}(s)}{E(s)} = -K_p \left(1 + \frac{1}{T_i s} \right) \quad (2)$$

where $V_{\text{con1}}(s)$ and $E(s)$ are the Laplace transforms of $v_{\text{con1}}(t)$ and $e(t)$; $e(t)$ is the error between reference and output; K_p and T_i are the control parameters. We can likewise write the equation for the slave.

We assume that the converter operates in continuous conduction mode and diodes D_1 and D_2 are always in complementary state to S_1 and S_2 . Consequently, the state equations of the converter stage of Fig. 1 are

$$\begin{cases} \dot{x}_1 = -\frac{1}{L_1} \left[(r_{L1} + \frac{Rr_c}{R+r_c})x_1 + \frac{Rr_c}{R+r_c}x_2 + \frac{R}{R+r_c}x_3 \right] + q_1 V_{in} \\ \dot{x}_2 = -\frac{1}{L_2} \left[\frac{Rr_c}{R+r_c}x_1 + (r_{L2} + \frac{Rr_c}{R+r_c})x_2 + \frac{R}{R+r_c}x_3 \right] + q_2 V_{in} \\ \dot{x}_3 = \frac{1}{C(R+r_c)}(Rx_1 + Rx_2 - x_3) \end{cases} \quad (3)$$

where x_1, x_2, x_3 are the converter state variables defined as

$$[x_1 \ x_2 \ x_3] = [i_{L1} \ i_{L2} \ v_c] \quad (4)$$

and q_1 and q_2 are the switching function decided by the controller. They are time varying functions given by

$$q_i(t) = \begin{cases} 1, & \text{if } v_{\text{coni}} \geq V_{\text{ramp}}, \\ 0, & \text{if } v_{\text{coni}} < V_{\text{ramp}}. \end{cases} \quad (5)$$

Depending upon the feedback circuit in Figs. 1(b) and (c), we have

$$\frac{dv_{\text{con1}}}{dt} = -K_1 \frac{dv_c}{dt} - \frac{K_1}{\tau_{F1}} v_c + \frac{K_1}{\tau_{F1}} V_{\text{ref}} \quad (6)$$

$$\begin{aligned} \frac{dv_{\text{con2}}}{dt} &= -K_2 \frac{dv_c}{dt} - \frac{K_2}{\tau_{F2}} v_c + K_2 K_i \left(\frac{di_{L1}}{dt} - \frac{di_{L2}}{dt} \right) \\ &+ \frac{K_2}{\tau_{F2}} (i_{L1} - i_{L2}) + \frac{K_2}{\tau_{F2}} V_{\text{ref}} \end{aligned} \quad (7)$$

where K_1 and K_2 are the proportional coefficients, τ_{F1} and τ_{F2} are the integral coefficients, K_i is the current sharing coefficient, and V_{ref} is the reference voltage (expected output voltage). In circuit terms, $K_1 = R_{F1}/R_1$, $\tau_{F1} = R_{F1}C_{F1}$, $K_2 = R_{F2}/R_2$, $\tau_{F2} = R_{F2}C_{F2}$, $K_i = R_F R_s / R$, where

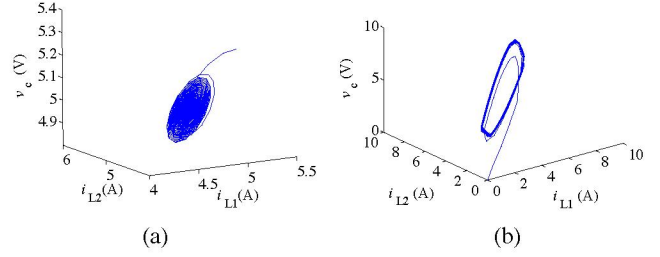


Fig. 2. Trajectory of paralleled buck converters from different initial condition for $K_1 = K_2 = 3$, $\tau_{F1} = \tau_{F2} = 1/\omega_0$, $K_i = 1$. (a) Trajectory converging toward stable operation for the initial value $X_0 = [5.2, 5, 4.8]$; (b) trajectory converging toward limit cycle for the initial value $X_0 = [0, 0, 0]$.

R_s is the current sensing resistance. Equations (6) and (7), together with (3), form the complete set of state equations of the system. It is a fifth order system.

III. BASINS OF ATTRACTION

In this section, we begin our investigation of the basins of attraction of the operation orbits. Our simulations are based on the state equations derived in the foregoing section and hence are exact cycle-by-cycle simulations. We are primarily concerned with the system stability in relation to the initial condition X_0 (X refers to the converter state variables), feedback parameters of the PI controller K_1 , K_2 , τ_{F1} , τ_{F2} and current sharing coefficient K_i . The circuit parameters and component values are listed in Table I.

TABLE I
COMPONENT VALUES USED IN SIMULATIONS

Circuit Components	Values
Switching Period T_s	10 μ s
Input Voltage V_{in}	12 V
Reference Voltage V_{ref}	5 V
Ramp Voltage V_L, V_U	3 V, 8 V
Inductance L_1 , ESR r_{L1}	55 μ H, 0.01 Ω
Inductance L_2 , ESR r_{L2}	60 μ H, 0.05 Ω
Capacitance C , ESR r_c	126 μ F, 0 Ω
Load Resistance R	0.5 Ω
Current sensing Resistance R_s	0.01 Ω

We choose an initial point, start the simulation and observe the steady-state trajectory. The expected equilibrium orbit is centered around $X_e = [5 \ 5 \ 5]$ corresponding to the values shown in Table I. Figure 2 (a) shows that the system will be converging to the stable equilibrium orbit if there is a small disturbance near the orbit. Under the same controller, but with initial point at the origin, Fig. 2 (b) shows the system converging to a limit cycle or other attractors, which can be considered “unstable” by engineers as it is not the desired orbit. Thus, there are more than one attractor in this system [8], [9]. The steady-state behavior of the system depends on where it starts. The basins of attraction are therefore important.¹

¹For the single converter case, stability was studied without reference to initial condition. In fact, this phenomenon was not found in single converters.

In the following, we find the basin boundaries numerically in relation to initial point X_0 , and determine how they are affected by the controller parameters K_1 , K_2 , τ_{F1} and τ_{F2} . Figures 3 (a) and (b) are basins of attraction presented on the i_{L1} - i_{L2} plane for different feedback coefficients K_1 and K_2 . Note that v_{c0} is 5V for this set of simulations. (In fact, the phenomenon is unaffected by the initial output voltage value, as we will elaborate later.) The expected equilibrium orbit is centered around the middle of the diagram. The yellow region is the basin corresponding to the desired operating orbit, whereas the blue region is the basin corresponding to attractors other than the desired orbit. Thus, if the system starts from the blue region, it will not converge to the expected operating orbit. Furthermore, we observe that the yellow region diminishes as proportional coefficients K_1 , K_2 increase; and vice versa. For large K_1 and K_2 , the yellow region subsides and the desired operating orbit is almost never stable. For small K_1 and K_2 , the blue region subsides and the desired operating orbit is almost always stable. In practice, K_1 and K_2 determine the response speed of the system [7]. We clearly see the limitation on selecting K_1 and K_2 so as to maintain stability for a wider basin of attraction.

Figures 3 (c) and (d) are basins of attraction in the i_{L1} - i_{L2} plane for different integral coefficients τ_{F1} and τ_{F2} . Normally, $1/\tau_{F1}$ and $1/\tau_{F2}$ should be near the corner frequency to get a stable compensation and fast response [7], [10]. Here, we compare $1/\tau_{F1}$ and $1/\tau_{F2}$ with the system inherent corner frequency ω_0 , which is defined as $\omega_0 = 1/\sqrt{LC}$, where L is the average value of L_1 and L_2 . The general trend of the variation of the basin boundaries is similar to Figs. 3 (a) and (b). As τ_{F1} and τ_{F2} decrease, the system goes from being globally stable to partially stable, and eventually unstable.

Furthermore, we present the case where the currents are maintained equal initially but the initial output voltage assumes a value different from the desired one. Figure 4 shows the basin of attraction in the v_c - i_{L1} plane. We observe similar trends with the variation of the control parameters.

IV. CAUTIONS ON STABILITY INFORMATION AND STABILITY BOUNDARIES

From the above results, an important conclusion can be made. The stability of the operating orbit can not be determined purely from the linear model or any method that tests stability by perturbing near the operating orbit. Stability information can be unreliable since global stability is not generally guaranteed from local stability tests. In general, we get different stability boundaries for different initial conditions.

The stability boundaries for the parallel connected buck converter system are shown in Figs. 5, 6 and 7, corresponding to two initial points. One is the origin $X_0 = [0, 0, 0]$, and the other is a point near the equilibrium orbit, i.e., near $X_0 = [5.2, 5, 4.8]$. The curve divides the parameter space into stable region (lower) and unstable region (upper). Thus, as we move across the boundary curve in any specific parameter space, the system changes from being stable to unstable, or vice versa. In Fig. 5 (a), K_1 and K_2 almost exponentially

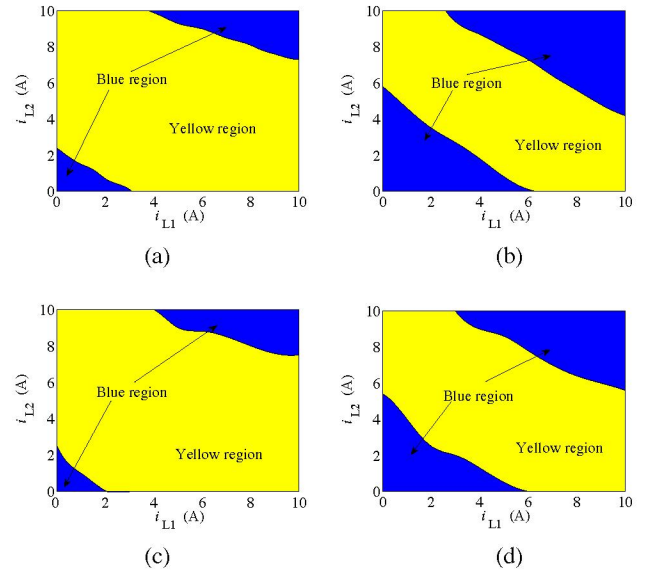


Fig. 3. Basins of attraction for different feedback parameters. Yellow region is the basin of attraction of the desired operating orbit. Blue region is the basin of attraction of attractors other than the desired operating orbit. (a) $K_1 = K_2 = 2.5$, $\tau_{F1} = \tau_{F2} = 1/\omega_0$, $K_i = 1$, $v_{c0} = 5$; (b) $K_1 = K_2 = 3.5$, $\tau_{F1} = \tau_{F2} = 1/\omega_0$, $K_i = 1$, $v_{c0} = 5$; (c) $K_1 = K_2 = 3$, $\tau_{F1} = \tau_{F2} = 1.03/\omega_0$, $K_i = 1$, $v_{c0} = 5$; (d) $K_1 = K_2 = 3$, $\tau_{F1} = \tau_{F2} = 0.95/\omega_0$, $K_i = 1$, $v_{c0} = 5$.

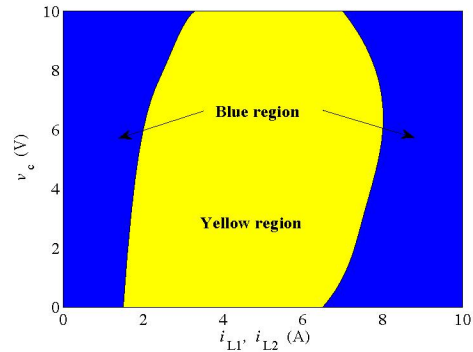
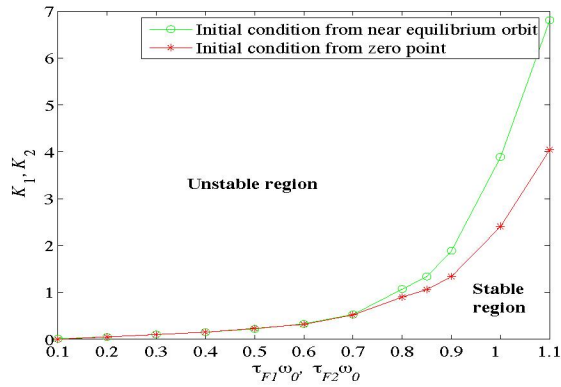


Fig. 4. Basin of attraction for different v_c and i_{L1} , i_{L2} for $K_1 = K_2 = 3$, $\tau_{F1} = \tau_{F2} = 1/\omega_0$, $K_i = 1$.

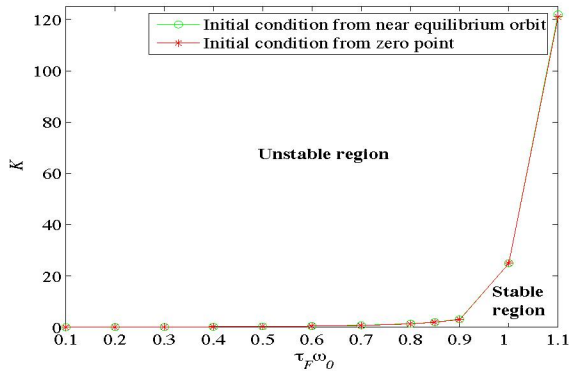
increase with $\tau_{F1}\omega_0$, $\tau_{F2}\omega_0$. Also, the gap between the two boundaries widens as $\tau_{F1}\omega_0$ and $\tau_{F2}\omega_0$ increase. Within the gap, coexisting attractors exist and stability information may be unreliable. It should be noted that the coexisting attractors do not exist in single buck converters, as shown in Fig. 5 (b), where the two boundary curves overlap in the parameter space.

Figure 6 shows the effect of the current sharing parameter K_i . When K_i is small, the two boundary curves are basically consistent. The gap widens as K_i increases, again indicating the existence of coexisting attractors. This shows that the coupling coefficient affects the complexity of the system behavior.

Finally, Fig. 7 shows the effects of changing the size of inductors L_1 and L_2 . We fix the difference of L_1 and L_2 , and maintain the system in continuous conduction mode (CCM).



(a)



(b)

Fig. 5. Stability boundaries of feedback parameters in (a) two paralleled buck converters in $\tau_{F1}\omega_0, \tau_{F2}\omega_0 - K_1, K_2$ plane for $K_i = 1$; (b) single buck converter in $\tau_F\omega_0 - K$ plane.

From the figure, we observe that the coexisting attractors exist when the inductors become small. Intuitively when the inductors are small, the system bandwidth becomes wide, admitting more high-frequency components in the feedback loop, hence becoming more prone to instability.

V. CONCLUSIONS

This paper studies the coexisting attractors in paralleled buck converters under master-slave current sharing and proportional-integral control. The system will be either stable or oscillatory depending on the initial condition. The implication of this finding is relevant to practical operation of the system since stability information obtained from linear models or any method that involves perturbation around the operating point can be unreliable. Specifically, stability information obtained from linear methods has been shown over-optimistic. In fact, the basin of attraction of an operating orbit is an important piece of design information, and stability boundaries in parameter space have to be interpreted in conjunction with the initial conditions. Different initial conditions may give rise to different stability boundaries. In this paper, we have reported the phenomenon and illustrated the effects of different parameters by presenting the numerical basins of attraction and specific stability boundaries.

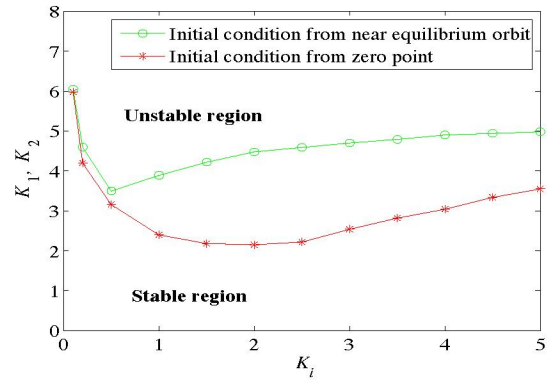


Fig. 6. Stability boundary of feedback parameters K_i versus K_1, K_2 for $\tau_{F1} = \tau_{F2} = 1/\omega_0$.

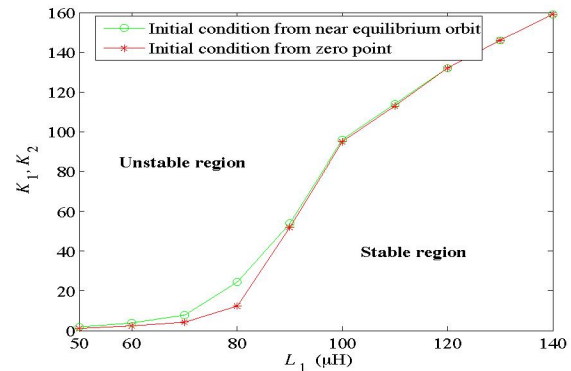


Fig. 7. Stability boundary of feedback parameters K_1, K_2 in relation to L_1 for $\tau_{F1} = \tau_{F2} = 1/\omega_0, K_i = 1$.

ACKNOWLEDGMENTS

This work was supported by Hong Kong Research Grants Council under a CERF project (Ref. PolyU 5237/04E).

REFERENCES

- [1] V. J. Thottuvelil and G. C. Verghese, "Analysis and control of paralleled dc/dc converters with current sharing," *IEEE Trans. Power Electron.*, vol. 13, no. 4, pp. 635–644, July 1998.
- [2] J. Rajagopalan, K. Xing, Y. Guo, F. C. Lee, and B. Manners, "Modeling and dynamic analysis of paralleled DC/DC converters with master-slave current sharing control," *Proc. IEEE APEC'96*, pp. 678–684, 1996.
- [3] Y. Panov, J. Rajagopalan, and F. C. Lee, "Analysis and design of N paralleled DC-DC converters with master-slave current-sharing control," *Proc. IEEE APEC'97*, pp. 436–442, 1997.
- [4] K. Siri, C. Q. Lee, and T. F. Wu, "Current distribution control for parallel connected converters: Part I and Part II," *IEEE Trans. Aerospace Electron. Syst.*, vol. 28, no. 3, pp. 829–851, July 1992.
- [5] C. K. Tse, *Complex Behavior of Switching Power Converters*, Boca Raton: CRC Press, 2003.
- [6] H. H. C. Iu and C. K. Tse, "Bifurcation behaviour of parallel-connected buck converters," *IEEE Trans. Circ. Syst. I*, vol. 48, no. 2, pp. 233–240, 2001.
- [7] K. Ogata, *Modern Control Engineering*, New York: Prentice Hall, 1997.
- [8] S. Banerjee and G. C. Verghese (Eds.), *Nonlinear Phenomena in Power Electronics: Attractors, Bifurcations, Chaos, and Nonlinear Control*, New York: IEEE Press, 2001.
- [9] G. Pegna, R. Marrocu, R. Tonelli, and F. Meloni, "Experimental definition of the basin of attraction for Chua's circuit," *Int. J. Bifur. Chaos*, vol. 10, no. 5, pp. 959–970, 2003.
- [10] G. C. Chryssis, *High-Frequency Switching Power Supplies: Theory and Design*, New York: McGraw-Hill, 1989.